PHYSICAL REVIEW B VOLUME 28, NUMBER 12 15 DECEMBER 1983

Surface segregation in simple metal alloys: An electronic theory

R. N. Barnett, Uzi Landman, and C. L. Cleveland
School of Physics, Georgia Institute of Technology, Atlanta, Georgia 30332
(Received 1 August 1983)

Surface segregation in simple-metal random binary alloys is studied via an electronic theory based on local ionic pseudopotentials and a linear-electron-response model appropriate for semi-infinite systems. Segregation of the larger species ions to the surface layer and (in most cases) a nonmonotonic layer concentration profile are predicted. The segregation of the larger species ions to the surface layer is driven by single-particle terms (Hartree-energy terms) in the total-energy expansion. These single-particle energy terms are independent of coordination number and relative positions of the ions but depend on the position of the surface layer relative to the inhomogeneous zeroth-order electron density at the metal surface, thus giving rise to crystal-face specificity. The concentration in deeper layers is determined primarily by effective interionic interactions. The electronic theory is compared with a nearest-neighbor pair-bond model, and it is concluded that the pair-bond model is not applicable to surface segregation in simple-metal alloys. The alloys considered in this paper are composed of the alkali metals K, Rb, and Cs. Concentration profiles as functions of temperature are presented for the (100) and (110) surfaces.

I. INTRODUCTION

Surface segregation is the enrichment of the concentration of one component at the surface of an alloy. This phenomena is of great interest since the surface composition affects a number of properties such as oxidation and corrosion, catalysis, chemisorption, wear, and electrical and mechanical properties of thin films. Recent experiments, employing modern surface-science techniques such as Auger-electron spectroscopy,[1] ultraviolet-photoelectron spectroscopy,[2] x-ray-photoemission spectroscopy,[3] low-energy ion scattering,[4] and atom-probe field-ion microscopy[5] have provided a wealth of detailed information on surface-segregation systems. These studies present evidence for a dependence of the surface composition on bulk composition, surface crystallography, and temperature. In some cases multilayer segregation and a nonmonotonic concentration profile[5] (i.e., oscillations in the composition as a function of depth) are indicated.

The possibility of surface segregation was predicted first by Gibbs[6] using thermodynamic arguments where the reduction of the surface energy serves as the driving force. More recent theories are of the pair-bond type[7] in which surface bond breaking provides the driving force, and some theories include strain energy due to a mismatch in the atomic sizes,[8] in which case minimization of the bulk strain energy provides an additional driving force. Recently there have also been several efforts to develop electronic theories of surface segregation in transition-metal alloys based on the tight-binding approximation.[9] A different approach is that of Muscat[10] in which a cluster of muffin-tin potentials is embedded at the surface or bulk of a free-electron gas; it was found in this study that the presence of the surface potential, rather than the number, positions, or species of neighboring atoms, plays the dominant role in surface segregation.

Theoretical treatment of alloy systems using band-structure or density-functional methods, sometimes in conjunction with the coherent-potential approximation and its variants, have, in general, been employed for calculation of the electronic densities of states of nonperiodic solids.[11] The application of these methods to calculations of formation energies of bulk alloys is quite difficult.[12] Furthermore the use of these methods in studies of surface properties of metal alloy systems is prohibitively complex, particulary for disordered systems. Thus it is desirable to construct a theoretical formulation which would allow systematic studies of surface properties and the physical origins of segregation in such systems. In the case of simple-metal (*sp*-bonded) alloys, pseudopotential theory in conjunction with linear-response, or second-order perturbation theory, has been applied with notable success in calculations of bulk-alloy formation energies (heats of mixing).[13]

The purpose of this paper is to present an electronic theory of surface segregation in simple, i.e., *sp*-bonded, metals. Our theory is based on the use of local ionic pseudopotentials and a linear-response model appropriate for a semi-infinite metal.[14] The formalism is given in Sec. II, and in Sec. III we present and discuss the results (layer composition versus temperature for different bulk compositions) and compare the predictions of our theory with those of a simple pair-bond—type theory. We find that the dominant factors which determine the composition of the surface layer are "single-particle" terms, i.e., terms in the total-energy expansion which depend on the position and species of an individual atom with respect to the inhomogenous electron-gas density in the surface region. In this respect our results are similar to those of Muscat[10] mentioned above. However, the composition of succeeding layers is determined primarily by interionic interactions, and in some cases we find a nonmonotonic concen-

 ©1983 The American Physical Society

tration profile. The larger species always segregates to the surface layer, segregation is greater for (100) than for (110) surfaces, and depends on temperature and bulk composition. The present study is limited to homovalent alloys consisting of the alkali metals K, Rb, and Cs. Work now in progress will deal with more technologically important (and more difficult to treat theoretically) simple-metal alloys such as Al-Li, Al-Mg, etc. In addition, we do not consider effects due to elastic strain and/or surface relaxation. These issues as well as local ordering effects will be discussed elsewhere.

II. THEORY

A. Free energy

Consider a semi-infinite solid solution composed of A and B atoms. The average concentration of species A is $\bar{x}$, and the concentration in the nth crystalline layer parallel to the surface is $x_n=\bar{x}+\Delta x_n$. The total (ground-state) energy of the system will depend on layer concentrations,

$$E_T=E_T(\bar{x},\{\Delta x_n\}) . \tag{1}$$

The heat of mixing is defined to be the difference between the total energy of the solid solution and that of a mechanical mixture of the pure species,[15]

$$H_m(\bar{x},\{\Delta x_n\})=E_T(\bar{x},\{\Delta x_n\})-\bar{x}E_T(\bar{x}=1) -(1-\bar{x})E_T(\bar{x}=0) . \tag{2}$$

The free energy of mixing can be approximated by

$$F_m(T,\bar{x},\{\Delta x_n\})=H_m(\bar{x},\{\Delta x_n\})-TS_m(\bar{x},\{\Delta x_n\}) , \tag{3a}$$

where T is the temperature, and

$$S_m(\bar{x},\{\Delta x_n\})=-k_B\sum_n [(\bar{x}+\Delta x_n)\ln(\bar{x}+\Delta x_n) +(1-\bar{x}-\Delta x_n)\ln(1-\bar{x}-\Delta x_n)] \tag{3b}$$

is the ideal entropy of mixing of the solid solution. In writing Eqs. (3) we have neglected any excess vibrational energy and entropy and we have assumed that the arrangement of species A and B within a given layer is completely random.

The equilibrium concentration profile is found by minimizing the free energy with respect to layer concentrations, subject to the constraint that the average concentration $\bar{x}$ does not change. We define a surface region consisting of N_s layers, and require the concentration to be uniform outside this region, i.e.,

$$x_n=\bar{x}+\Delta x_n \quad \text{for } 1\le n\le N_s , \tag{4a}$$

$$x_n=\bar{x}+\Delta x_b \quad \text{for } N_s+1\le n\le N_L , \tag{4b}$$

where N_L is the total number of layers (the limit $N_L\to\infty$ will be taken). The constraint is

$$\Delta x_b=-(N_L-N_s)^{-1}\sum_{n=1}^{N_s}\Delta x_n . \tag{5}$$

The N_s coupled differential equations which determine the equilibrium configuration (layer-concentration profile) are

$$\frac{\partial F_m}{\partial\Delta x_n}-(N_L-N_s)^{-1}\frac{\partial F_m}{\partial\Delta x_b}=0, \quad 1\le n\le N_s . \tag{6}$$

B. Pseudopotential linear-response formulation

The calculation of the surface-concentration profile from Eq. (6) requires an expression for the total energy which depends explicitly on the atomic species and their concentration in the surface-region layers and in the bulk. We have previously obtained an expression for the total energy of a semi-infinite simple metal using local model ionic pseudopotentials and linear-response theory.[14] In this section we will outline the theory presented in Ref. 14 and apply it to the surface segregation problem.

The semi-infinite metal is represented by an interacting electron gas in the presence of a truncated neutralizing positive background (jellium model), to which we add a term which replaces the jellium positive background by a lattice of discrete ions. The electronic Hamiltonian is written as

$$H=H^0+\sum_i w_i , \tag{7}$$

where H^0 is the many-body Hamiltonian of the electron-jellium system; the ground-state energy E^0 and electron density $\rho^0(\vec{r})$ of the semi-infinite electron-jellium system are given in the seminal study by Lang and Kohn.[16] The potentials associated with individual ions $w_i(\vec{r})$ are given by

$$w_i(\vec{r})=V_P(\beta_i;|\vec{r}-\vec{r}_i|)-N^{-1}Z(\beta_i)V_+(\vec{r}) , \tag{8}$$

where β_i is the species of the ion at position $\vec{r}_i$, $V_P(\beta,r)$ and $Z(\beta)$ are the bare ionic pseudopotential and valence charge, respectively, of the ion of species β, $N=\sum_i Z(\beta_i)$ is the total number of conduction electrons, and $V_+(\vec{r})$ is the potential due to the neutralizing positive background charge. Thus, $w_i(\vec{r})$ is a neutral perturbation which results from replacing a part of the positive background with an individual ion at site $\vec{r}_i$.

With the use of the coupling-constant integration method and assuming linear response, the total energy of the semi-infinite metal is given by[14]

$$E_T=E^0+\sum_i\int d^3r\,\rho^0(\vec{r})w_i(\vec{r}) +\tfrac{1}{2}\left[\sum_{i,j}\int d^3r\,\rho_i(\vec{r})w_j(\vec{r})\right]+E_M , \tag{9}$$

where $\rho_i(\vec{r})$ is the screening electron density induced by the potential $w_i(\vec{r})$, and E_M is the Madelung energy of the ions. The major task in evaluating E_T for an arbitrary arrangement of ions of different species is to obtain a self-consistent solution for the screening electron densities $\rho_i(\vec{r})$. Linear-response theory yields[14] a pair of coupled integral equations,

$$\rho_i(\vec{r})=\int d^3r'\alpha_0(\vec{r},\vec{r}')[w_i(\vec{r}')+\phi_i(\vec{r}')]\ , \tag{10a}$$

$$\phi_i(\vec{r})=\int d^3r'[1-G(\vec{r},\vec{r}')]\rho_i(\vec{r}')\frac{e^2}{|\vec{r}-\vec{r}'|}\ , \tag{10b}$$

where $\alpha_0(\vec{r},\vec{r}')$ is the random-phase-approximation (RPA) response function and $\phi_i(\vec{r})$ is the self-consistent effective potential due to $\rho_i(\vec{r})$, which includes exchange-correlation effects through the local-field correction $G(\vec{r},\vec{r}')$.[17,14] In our calculations we use the infinite-barrier-response model developed in Ref. 14, i.e., α_0 is the RPA response function for a free-electron gas confined to the half-space $z\geq 0$ and the local-field correction $G(\vec{r},\vec{r}')$ is approximated by $G(|\vec{r}-\vec{r}'|)$. The details of this response model are discussed in Ref. 14. This response model has also been used to predict the relaxed structure of the low-index surfaces of Al and Na,[18] yielding good agreement with available experimental results including multilayer relaxation in Al(110).

For notational convenience the layer positions are given by

$$z_n=z_0+(n-\tfrac{1}{2})d,\quad n=1,2,\ldots \tag{11}$$

where $z_0=3\pi/8k_F$, $\hbar k_F$ is the Fermi momentum, and d is the interlayer spacing. In this response model $\rho_n(\vec{r})=0$ for $z\leq 0$; thus we are able to define symmetrized quantities,

$$w_{is}(\vec{r})=w_i(R,|z|) \tag{12a}$$

and

$$\rho_{is}(\vec{r})=\rho_i(R,|z|)\ , \tag{12b}$$

where $\vec{r}=(\vec{R},z)$, $\vec{R}$ is a two-dimensional (2D) vector in the surface plane. With the use of these symmetrized quantities, we are able to evaluate the second-order [band-structure (BS)] energy term entirely in reciprocal space. Thus, the third term in Eq. (9) becomes

$$E_{\rm BS}=\tfrac{1}{4}\sum_{i,j}(2\pi)^{-3}\int d^3q\, e^{i\vec{Q}\cdot(\vec{R}_i-\vec{R}_j)}\rho_{is}(\vec{q})w_{js}(\vec{q})\ , \tag{13}$$

where $\rho_{is}(\vec{q})$ and $w_{is}(\vec{q})$ are the three-dimensional (3D) Fourier transforms of $\rho_{is}(\vec{r})$ and $w_{is}(\vec{r})$, and $\vec{q}=(\vec{Q},q_z)$ is a 3D reciprocal-space vector. The screening electron density $\rho_{is}(\vec{q})$ is obtained as a function of q_z for a given $|\vec{Q}|$, layer, and atomic species by solving a single one-dimensional (1D) integral equation, as discussed in Ref. 14.

We will now use Eqs. (9) and (13) in the surface-segregation problem. The theory described in the following is similar to that developed by Inglesfield[19] for application to disordered alloys, except that we will allow for variations in concentration in the z direction. For the purpose of the present study we consider only homovalent alloys, $Z(A)=Z(B)=Z$, and assume that the ion positions are lattice sites of a truncated bulk crystal (no lattice relaxation at the surface and no distortion around impurity ions); thus E_M, the Madelung energy, is independent of $\{\Delta x_n\}$. However, we do not assume Vegard's law, i.e., we minimize the total energy of a homogenous bulk random alloy with respect to density to determine the lattice constant and (bulk) total energy for a particular concentration $\bar{x}$.

It is convenient to define average and difference potentials for layers,

$$\bar{w}_n(\vec{r})=\bar{x}V_P(A,(r^2-z_n^2)^{1/2})+(1-\bar{x})V_p(B,(r^2-z_n^2)^{1/2})-N^{-1}ZV_+(z) \tag{14}$$

and

$$\Delta w_n(\vec{r})=V_p(A,(r^2-z_n^2)^{1/2})-V_p(B,(r^2-z_n^2)^{1/2})\ , \tag{15}$$

where z_n [Eq. (11)] is the z coordinate of the nth layer. Symmetrized reciprocal-space potentials $\bar{w}_{ns}(\vec{q})$, $\Delta w_{ns}(\vec{q})$, and their corresponding screening-electron densities $\bar{\rho}_{ns}(\vec{q})$ and $\Delta\rho_{ns}(\vec{q})$ are defined in analogy to Eqs. (12) (with $\vec{R}_i=\vec{0}$).

With the use of the definitions given above, the second term on the right-hand side (rhs) of Eq. (9) (the first-order or "Hartree" energy) is

$$\sum_i\int d^3r\,\rho^0(\vec{r})w_i(\vec{r})=\sum_n[\bar{E}_H(n)+\Delta x_n\,\Delta E_H(n)]\sum_{i(n)}(1)\ , \tag{16}$$

where

$$\bar{E}_H(n)=\int d^3r\,\rho^0(z)\bar{w}_n(\vec{r})\ , \tag{17}$$

$$\Delta E_H(n)=\int d^3r\,\rho^0(z)\Delta w_n(\vec{r})\ , \tag{18}$$

and where $i(n)$ specifies a lattice site in layer n.

The third term on the rhs of Eq. (9), i.e., the band-structure energy, Eq. (13), depends on the distribution of the atomic species within the layers as well as on the layer concentrations. Every site in a given layer is equivalent, i.e., each site in the layer sees on the average the same distribution of A and B species around it regardless of whether that site is occupied by an A or B atom. Thus the band-structure energy can be written

$$\begin{aligned}E_{\rm BS}=&\frac{1}{4}\frac{1}{(2\pi)^3}\int d^3q\sum_{n,m}[\bar{\rho}_{ns}(\vec{q})+\Delta x_n\,\Delta\rho_{ns}(\vec{q})][\bar{w}_{ms}(\vec{q})+\Delta x_m\Delta w_{ms}(\vec{q}]\sum_{i(n),j(m)}{}'e^{i\vec{Q}\cdot(\vec{R}_{i(n)}-\vec{R}_{j(m)})}\\&+\frac{1}{4}\frac{1}{(2\pi)^3}\int d^3q\sum_n\{(\bar{x}+\Delta x_n)[\bar{\rho}_{ns}(\vec{q})+(1-\bar{x})\Delta\rho_{ns}(\vec{q})][\bar{w}_{ns}(\vec{q})+(1-\bar{x})\Delta w_{ns}(\vec{q})]\\&+(1-\bar{x}-\Delta x_n)[\bar{\rho}_{ns}(\vec{q})-\bar{x}\,\Delta\rho_{ns}(\vec{q})][\bar{w}_{ns}(\vec{q})-\bar{x}\,\Delta w_{ns}(\vec{q})]\}\sum_{i(n)}1\ .\end{aligned} \tag{19}$$

The primed sum omits the $j(m)=i(n)$ terms, and the second integral in Eq. (19) results from the fact that the potential at a given site, and thus the "self-interaction energy" $\int d^3r\,\rho_i(\vec{r})w_i(\vec{r})$, cannot be expressed in terms of the averaged quantities for a layer.

For a Bravais lattice,

$$\sum_{i(n),j(m)} e^{i\vec{Q}\cdot(\vec{R}_{i(n)}-\vec{R}_{j(m)})}=N_A\sum_{\vec{G}}\frac{(2\pi)^2}{A_0}\delta(\vec{Q}-\vec{G})(s_{\vec{G}})^{n-m}\,, \tag{20}$$

where $N_A=\sum_{i(n)}1$ is the number of ions in a layer, A_0 is the area per surface atom, $\vec{G}$ is a 2D reciprocal-lattice vector, and $s_{\vec{G}}=e^{i\vec{G}\cdot\Delta\vec{R}}$, where $\Delta\vec{R}$ is the registry shift between adjacent layers. With the use of Eq. (20) and rearranging terms in Eq. (19), the band-structure energy can be written as

$$\begin{aligned}N_A^{-1}E_{\rm BS}=&\frac{1}{4A_0}\sum_{n,m}\frac{1}{2\pi}\sum_{\vec{G}}\int dq_z(s_{\vec{G}})^{n-m}[\bar{\rho}_{ns}(\vec{G},q_z)\bar{w}_{ms}(\vec{G},q_z)+\Delta x_n\,\Delta\rho_{ns}(\vec{G},q_z)\bar{w}_{ms}(\vec{G},q_z)\\&+\Delta x_m\,\bar{\rho}_{ns}(\vec{G},q_z)\Delta w_{ms}(\vec{G},q_z)+\Delta x_n\,\Delta x_m\,\Delta\rho_{ns}(\vec{G},q_z)\Delta w_{ms}(\vec{G},q_z)]\\&+\tfrac{1}{4}\sum_n(2\pi)^{-3}\int d^3q(\bar{x}+\Delta x_n)(1-\bar{x}-\Delta x_n)\Delta\rho_{ns}(\vec{q})\Delta w_{ns}(\vec{q})\,.\end{aligned} \tag{21}$$

Substituting Eqs. (16)—(18) and (21) into the total-energy expression yields

$$N_A^{-1}E_T=N_A^{-1}\bar{E}_T+\sum_n f_n\,\Delta x_n+\tfrac{1}{2}\sum_{n,m}\phi_{nm}\,\Delta x_n\,\Delta x_m\,, \tag{22}$$

where the terms on the rhs are defined and discussed below.

(a) $\bar{E}_T$ is the total energy of a uniform ($\Delta x_n\equiv 0$) semi-finite solid solution of concentration $\bar{x}$ given by

$$\begin{aligned}N_A^{-1}\bar{E}_T=&N_A^{-1}E^0+\sum_n\bar{E}_H(n)+\tfrac{1}{4}\sum_{n,m}(2\pi A_0)^{-1}\sum_{\vec{G}}\int dq_z\bar{\rho}_{ns}(\vec{G},q_z)\bar{w}_{ms}(\vec{G},q_z)\\&+\tfrac{1}{4}\sum_n(2\pi)^{-3}\int d^3q\,\bar{x}(1-\bar{x})\Delta\rho_{ns}(\vec{q})\Delta w_{ns}(\vec{q})\,.\end{aligned} \tag{23}$$

(b) f_n is the change in the total energy of the uniform solid solution resulting from replacing an atom of species B in the nth layer with an atom of species A. It can be regarded as an "impurity" formation energy and is given by

$$f_n=\Delta E_H(n)+\Delta E'_{\rm BS}(n)+(1-2\bar{x})\Delta E_s(n)\,, \tag{24}$$

where

$$\Delta E'_{\rm BS}(n)=\tfrac{1}{4}\sum_m(2\pi A_0)^{-1}\sum_{\vec{G}}(s_{\vec{G}})^{n-m}\int dq_z[\Delta\rho_{ns}(\vec{G},q_z)\bar{w}_{ms}(\vec{G},q_z)+\bar{\rho}_{ns}(\vec{G},q_z)\Delta w_{ms}(\vec{G},q_z)] \tag{25}$$

and

$$\Delta E_s(n)=\tfrac{1}{4}(2\pi)^{-3}\int d^3q\,\Delta\rho_{ns}(\vec{q})\Delta w_{ns}(\vec{q})\,. \tag{26}$$

The second term, $\Delta E'_{\rm BS}(n)$, depends explicitly on the average concentration $\bar{x}$ [through the definitions of $\bar{w}$ and $\bar{\rho}$; see Eq. (13)], while $\Delta E_H(n)$ and $\Delta E_s(n)$ depend on $\bar{x}$ only through the density parameter r_s which determines $\rho^0(z)$ and the lattice parameter and which is obtained by minimizing $\bar{E}_T$ with respect to density for a given $\bar{x}$. These two terms, $\Delta E_H(n)$ and $\Delta E_s(n)$, depend on the z coordinate of the layer but are otherwise independent of crystal structure. For sufficiently deep layers (large n) f_n is independent of layer number and is equal to the bulk value, $f_{\rm bulk}$, which can be calculated for an infinite solid solution. Since in the bulk case the calculation can be done entirely in reciprocal space and there are no sums over layers, this serves as a check on the accuracy of the calculations.

(c) ϕ_{nm} serves to couple the concentrations in layers n and m, and is given by

$$\phi_{nm}=\tfrac{1}{4}(2\pi A_0)^{-1}\sum_{\vec{G}}(s_{\vec{G}})^{n-m}\int dq_z[\Delta\rho_{ns}(\vec{G},q_z)\Delta w_{ms}(\vec{G},q_z)+\Delta\rho_{ms}(\vec{G},q_z)\Delta w_{ns}(\vec{G},q_z)]-2\delta_{n,m}\Delta E_s(n)\,, \tag{27}$$

where $\Delta E_s(n)$ is defined in Eq. (26). The only dependence of ϕ_{nm} on $\bar{x}$ is through the density parameter r_s. ϕ_{nm} becomes negligably small for large $|n-m|$, and for sufficiently deep layers ϕ_{nm} is equal to the bulk value, $\phi_{\rm bulk}(|n-m|)$, which also can serve as a check on the accuracy of the calculation.

We now return to the minimization of the free energy, or equivalently the free energy of mixing given by Eq. (3), with

respect to layer concentration, to find the surface-concentration profile. Substituting Eqs. (1)—(3) and Eq. (22) into Eq. (6) yields a set of nonlinear coupled algebraic equations for the Δx_n,

$$0=\sum_{m=1}^{N_s}\phi_{nm}\,\Delta x_m+(f_n-f_{\rm bulk})+k_BT\ln\left[\frac{(\bar{x}+\Delta x_n)(1-\bar{x})}{\bar{x}(1-\bar{x}-\Delta x_n)}\right],\quad 1\le n\le N_s\ . \tag{28}$$

In writing Eq. (28) we have taken the limit of an infinite number of layers, $N_L\to\infty$, so that Δx_b [see Eq. (5)] is negligable in the entropy term, $N_L/(N_L-N_s)=1$, and N_s is large enough so that $f_n=f_{\rm bulk}$ for $n>N_s$. [N_s must also be large enough so that $\Delta x_n=\Delta x_b$ for $n>N_s$; see Eqs. (4) and (5)]. The free energy of segregation, i.e., the difference between the free energy of the equilibrium configuration and that of the uniform solid solution, is

$$\begin{aligned}\Delta F_{\rm seg}=F_m(\bar{x},\{\Delta x_n\})-F_m(\bar{x},\{\Delta x_n\equiv 0\})=&\sum_{n=1}^{N_s}\Delta x_n\left[-(f_n-f_{\rm bulk})+\tfrac{1}{2}\sum_{m=1}^{N_s}\Delta x_m\phi_{nm}\right]\\&+k_BT\sum_{n=1}^{N_s}[\,(\bar{x}+\Delta x_n)\ln(\bar{x}+\Delta x_n)-\bar{x}\ln(\bar{x})\\&+(1-\bar{x}-\Delta x_n)\ln(1-\bar{x}-\Delta x_n)-(1-\bar{x})\ln(1-\bar{x})]\ .\end{aligned} \tag{29}$$

C. Pair-bond model

Before presenting our results in Sec. III we will discuss briefly a simple version of the pair-bond enthalpy formulation and contrast it with our pseudopotential linear-response formulation. In the pair-bond model the cohesive energy of the alloy is written as a sum over bonds,

$$E_c=\tfrac{1}{2}{\sum_{i,j}}'\epsilon_{ij}\ . \tag{30}$$

The cohesive energy is related to the total energy E_T by

$$E_c(\bar{x},\{\Delta x_n\})=E_T(\bar{x},\{\Delta x_n\})+N[\bar{x}E_I^A+(1-\bar{x})E_I^B]\ , \tag{31}$$

where E_I^A and E_I^B are the ionization energies of the A and B atoms. The heat of mixing is thus

$$H_m=E_c(\bar{x},\{\Delta x_n\})-\bar{x}E_c(\bar{x}=1)-(1-\bar{x})E_c(\bar{x}=0)\ . \tag{32}$$

For a bulk alloy, assuming nearest-neighbor interactions only, the cohesive energy is given by

$$\frac{1}{N}E_c(\bar{x})=\frac{C}{2}[\bar{x}^2\epsilon_{AA}+(1-\bar{x})^2\epsilon_{BB}+2\bar{x}(1-\bar{x})\epsilon_{AB}]\ , \tag{33}$$

where C is the coordination number. If ϵ_{AA} and ϵ_{BB} do not depend on $\bar{x}$ then they can be obtained from the pure-species cohesive energy [experimental, or from Eq. (31) using a calculated E_T],

$$\epsilon_{AA}=\frac{2}{C}E_c(\bar{x}=1),\quad \epsilon_{BB}=\frac{2}{C}E_c(\bar{x}=0)\ . \tag{34}$$

The interspecies bond strength is written as

$$\epsilon_{AB}=\tfrac{1}{2}(\epsilon_{AA}+\epsilon_{BB})+\epsilon\ . \tag{35}$$

For an ideal solution $\epsilon=0$, but if the heat of mixing is known (again either an experimental or calculated bulk value), then

$$\epsilon(\bar{x})=[NC\bar{x}(1-\bar{x})]^{-1}H_m(\bar{x})\ . \tag{36}$$

The surface-segregation problem can be cast in the form of Eq. (28). We define the layer coordination number C_{nm} to be the number of nearest neighbors that an ion in layer n has in layer m (or vice versa). The formation energies are

$$f_n=\sum_{m=1}^{\infty}C_{nm}[(1-2\bar{x})\epsilon+\tfrac{1}{2}(\epsilon_{AA}-\epsilon_{BB})]\ , \tag{37}$$

and the layer-coupling matrix elements are

$$\phi_{nm}=-2C_{nm}\epsilon\ . \tag{38}$$

For a Bravais lattice $C_{nm}=C(\,|n-m|\,)$; the only nonzero C for bcc (100) layers is $C(1)=4$, and for bcc (110) layers the nonzero C's are $C(0)=4$ and $C(1)=2$. Thus, for bcc (100) and (110) surfaces only the surface layer has a formation energy different from the bulk, and there is no coupling beyond adjacent layers. In addition, the same-layer coupling term for (100) layers is zero. The pair-bond model can be extended to include interactions beyond nearest neighbors and to allow for different bond strengths near the surface, but it is difficult to uniquely determine the additional parameters. In any case, the pair-bond model cannot account for terms which arise from the direct and indirect interaction of a single ion with the inhomogenous electron gas (see Ref. 14).

III. RESULTS AND DISCUSSION

In this section the theory developed in Sec. II is applied to the simple-metal alloys $Rb_{\bar{x}}K_{1-\bar{x}}$, $Cs_{\bar{x}}K_{1-\bar{x}}$, and $Cs_{\bar{x}}Rb_{1-\bar{x}}$. The choice of ionic pseudopotentials and properties of the bulk alloys are discussed in Sec. III A. In Sec. III B we discuss the various contributions to the formation energy f_n and differences $f_n-f_{\rm bulk}$ using the $Cs_{\bar{x}}K_{1-\bar{x}}$ system as an example. We also discuss the layer-coupling matrix elements, ϕ_{nm} and differences between bulk and surface terms. The results of surface-segregation calculations, in the form of layer-concentration x_n—versus—temperature curves, are presented.

TABLE I. Parameters used in the calculations: r_c and u_c are the pseudopotential core radius and depth [see Eq. (39)], and r_s and $N^{-1}E_T$ are the electron-density parameters and bulk total energy per particle.

Metal	r_c	u_c	r_s	$N^{-1}E_T$ (Ry)
K	$3.033a_0$	0.5723	$4.861a_0$	−0.3891
Rb	$3.551a_0$	0.7273	$5.196a_0$	−0.3687
Cs	$4.112a_0$	0.8079	$5.625a_0$	−0.3449

A. Bulk properties

In general, the choice of a model pseudopotential is guided by the adequacy of the fit between certain calculated and measured material properties. When treating metal surfaces it is essential that the model yields the correct bulk lattice constant at zero pressure and reproduces, as well as possible with a limited number of parameters, the elastic properties of the bulk metal. In addition, if the model is applied to alloys, it is of utmost importance that the model also yield the correct total energy, and thus the correct cohesive energy, of the pure species.

The simplified Heine-Abarenkov[20] model pseudopotential has been used by a number of authors[13] to calculate properties (heat of mixing, phase diagrams, etc.) of alkali-metal alloys. We will use the form

$$V_p(\beta,r)=\begin{cases}\dfrac{-Z(\beta)e^2}{r}, & r\geq r_c(\beta)\\ \dfrac{-Z(\beta)e^2u_c(\beta)}{r_c(\beta)}, & r\leq r_c(\beta)\end{cases} \tag{39}$$

where $Z(\beta)$ is the charge of the ion of species β in units of the electron charge, e [$Z(\beta)=1$ for the alkali metals], and $r_c(\beta)$ and $u_c(\beta)$ are the core-radius and depth parameters. These parameters, r_c and u_c, are chosen to reproduce the lattice constant and bulk modulus of the pure species[21] and are given in Table I. The model pseudopotentials were used in Ref. 21 to calculate vacancy formation energy and volume, and yielded results in good agreement with experiment. We have verified that these potentials give the correct lattice constant by minimizing the total energy of the pure species with respect to the electron density parameter r_s; the resulting values of r_s and total energy per atom $N^{-1}E_T$ are also given in Table I. The calculated total-energy values agree with experiment[22] [see Eq. (31)] to within a fraction of 1% in each case. We have also verified that these pseudopotentials predict a bcc structure by comparing the total energies with those obtained by assuming fcc and hcp structures.

The results of minimizing the total energy of the random alloy systems with respect to r_s are summarized in Table II where we give results for concentrations $\bar{x}=0.1$, 0.5, and 0.9 (these are the bulk concentrations used in the surface-segregation calculations). The deviations from Vegard's law for volumes

$$r_s(\bar{x})=[\bar{x}r_s^3(1)+(1-\bar{x})r_s^3(0)]^{1/3}$$

are small and negative. The calculated values of the heat of mixing are all positive due to the structure-independent contributions[23]; the band-structure contribution can be positive or negative and are about an order of magnitude smaller than the structure-independent contribution in each case. The quantity $N^{-1}H_m/\bar{x}(1-\bar{x})$ shown in Table II is proportional to the alloy potential ϵ of the pair-bond model [see Eq. (36)]. This quantity is zero for an ideal solution and is constant for a regular solution pair-bond model. The qualitative behavior of $H_m(\bar{x})$ is in agreement with other calculations[24,25] and with liquid-alloy experimental results[26] regarding the asymmetry of $H_m(\bar{x})$ about $\bar{x}=0.5$. In particular, $H_m(\bar{x})/\bar{x}(1-\bar{x})$ is approximately a linear function of $\bar{x}$, except for the Cs-K system, and $H_m(\bar{x})/\bar{x}(1-\bar{x})$ increases with increasing concentration of the larger species. Yokokawa and Kleppa[26] have obtained approximate values of H_m for the solid solutions $Rb_{0.7}K_{0.3}$, $Cs_{0.5}K_{0.5}$, and $Cs_{0.5}Rb_{0.5}$ by extrapolation from their liquid-metal experimental results, and these values are compared to the results of several calculations[24] in Table I of Ref. 25. The calculated values reported there are all much greater than the experimental values, as are

TABLE II. Bulk alloy results: r_s is the electron-density parameter, E_T is the total energy, H_m is the heat of mixing, T_D is the calculated "disordering" temperature [Eq. (40)], and T_m is the melting temperature.

A_xB_{1-x}	r_s (a_0)	$N^{-1}E_T$ (Ry)	$N^{-1}H_m/\bar{x}(1-\bar{x})$ (Ry)	T_D (K)	T_m (K)
Rb_1K_9	4.896	−0.3869	0.0018	80	330
Rb_5K_5	5.034	−0.3785	0.0017	95	310
Rb_9K_1	5.165	−0.3706	0.0016	70	310
Cs_1K_9	4.948	−0.3839	0.0092	400	283
Cs_5K_5	5.267	−0.3652	0.0072	410	283
Cs_9K_1	5.556	−0.3487	0.0063	270	278
Cs_1Rb_9	5.242	−0.3662	0.0020	90	300
Cs_5Rb_5	5.418	−0.3563	0.0019	105	282
Cs_9Rb_1	5.584	−3.471	0.0017	75	293

ours. We get values of H_m which are about 2, 3.5, and 11 times the extrapolated experimental values for $Rb_{0.7}K_{0.3}$, $Cs_{0.5}K_{0.5}$, and $Cs_{0.5}Rb_{0.5}$, respectively. However, our values are generally lower than the other reported calculated values. The discrepancy between calculated and experimental values may be due to the assumption that the heat and entropy of mixing are independent of temperature which is made in Ref. 25 in extracting the solid solution H_m from liquid-alloy measurements as well as in the calculations, and the neglect of short-range order and lattice distortion in the calculations. The "disordering" temperature $T_D(\bar{x})$, below which the free energy of a mechanical mixture (clustered or segregated) of the pure species is lower than that of the *random* solid solution of concentration $\bar{x}$, is given by

$$T_D(\bar{x})=H_m(\bar{x},\{\Delta x_n=0\})/S_m(\bar{x},\{\Delta x_n=0\}) . \quad (40)$$

Values of $T_D(\bar{x})$ for alloys studied in this paper are also given in Table II. The assumption that the alloy is a random solid solution is invalid near and below $T=T_D(\bar{x})$. A correct treatment of the bulk heat of mixing and of surface segregation would require the inclusion of short-range order in both the energy and entropy terms,[27] which has only been accomplished in the context of simple pair-bond models[28] limited to nearest-neighbor bonds. Available phase diagrams[29] indicate that each of the alloy systems considered here [with the possible exceptions of K-Cs (Ref. 30)] form continous solid solutions near room temperature, but information regarding the presence and degree of short-range order is not available. Our results for Rb_xK_{1-x} and Cs_xRb_{1-x} are consistent with these experimental phase diagrams. The results for Cs_xK_{1-x} are not necessarily inconsistent with experiment since we have assumed a totally random solid solution; the inclusion of short-range order would certainly lower the predicted clustering (i.e., segregating) temperature.

B. Formation energies and layer-coupling matrix

In this section we discuss the formation energies f_n [Eq. (24)] and layer-coupling matrix ϕ_{nm} [Eq. (27)]. Table III lists the numerical values of the bulk formation energies f_{bulk} for the alloy systems which are treated in this paper, along with the contributions ΔE_H, ΔE_s and $\Delta E'_{\text{BS}}$ [Eqs. (18), (25), and (26), respectively]. The Hartree (first order in the ionic pseudopotentials) contribution ΔE_H is by far the largest in magnitude and is larger in the Cs-K alloys where the difference in ionic size (pseudopotential core radius or pure-species volume per atom) is larger than in either the Rb-K or Cs-Rb alloys. Also note that ΔE_H is positive and decreases as the concentration of the larger species increases. f_{bulk} is defined to be the change in energy of the A_xB_{1-x} alloy when one of the smaller B ions is replaced by a larger A ion. Thus we see that more energy is required to substitute a large ion in an alloy consisting primarily of smaller ions than vice versa. This is what one would expect based on elastic strain arguments; however, the mechanism involved is different here since the Hartree energy is independent of structure (relative positions of ions). The self-interaction difference ΔE_s is also structure independent and is relatively insensitive to concentration (when expressed in units of e^2k_F). The last contribution, $\Delta E'_{\text{BS}}$, is essentially a sum over effective ionic interactions. This term may be either positive or negative and decreases (or becomes more negative) as the concentration of the larger species increases.

The formation-energy difference f_n-f_{bulk} is the driving force which gives rise to surface segregation. The dependence of this quantity on layer number and on alloy composition is illustrated in Table IV using the Cs-K (100) alloy surfaces as an example. The formation-energy difference is always negative for the first layer, indicating that the larger species will segregate to the surface. The principal contribution to this first-layer energy difference is again the Hartree-energy term and results from the fact that the "zeroth-order" electron density $\rho^0(z)$ is smaller at the position of the first layer. In the second layer the Hartree and second-order (band-structure) contributions tend to cancel, and past the second layer all contributions are essentially zero, so that only the first layer has a significant formation-energy difference. This is similar to the simple nearest-neighbor pair-bond model in which $f_n-f_{\text{bulk}}=0$ for $n>1$ at low-index surfaces. However, we emphasize again that the mechanisms involved are not

TABLE III. Bulk formation energy, $f_{\text{bulk}}=\Delta E_H+(1-2\bar{x})\Delta E_s+\Delta E'_{\text{BS}}$ [see Eqs. (18) and (24)–(26)]. Units of energy are e^2k_F where $k_F=(9\pi/4)^{1/3}/r_s$ and $r_s(\bar{x})$ is given in Table II.

A_xB_{1-x}	ΔE_H (e^2k_F)	ΔE_s (e^2k_F)	$\Delta E'_{\text{BS}}$ (e^2k_F)	f_{bulk} (e^2k_F)	f_{bulk} (Ry)
Rb_1K_9	0.0262	−0.0018	0.0029	0.0277	0.0217
Rb_5K_5	0.248	−0.0018	0.0017	0.0265	0.0202
Rb_9K_1	0.0236	−0.0017	0.0006	0.0255	0.0190
Cs_1K_9	0.0673	−0.0076	0.0039	0.0651	0.0505
Cs_5K_5	0.0594	−0.0074	0.0002	0.0596	0.0435
Cs_9K_1	0.0534	−0.0071	−0.0026	0.0565	0.0390
Cs_1Rb_9	0.0371	−0.0024	−0.0004	0.0347	0.0254
Cs_5Rb_5	0.0347	−0.0024	−0.0012	0.0335	0.0238
Cs_9Rb_1	0.0327	−0.0024	−0.0019	0.0327	0.0224

TABLE IV. Contributions to the formation-energy difference for $Cs_{\bar{x}}K_{1-\bar{x}}$ alloys, (100) layers; $[f_n - f_{\text{bulk}}] = \Delta[\Delta E_H(n)] + (1-2\bar{x})\Delta[\Delta E'_{\text{BS}}(n)]$ where $\Delta[\Delta E_H(n)] = \Delta E_H(n) - \Delta E_H(\text{bulk})$, etc. [see Eqs. (18) and (24)–(26)]. Units of energy are e^2k_F, where $k_F = (9\pi/4)^{1/3}/r_s$ and $r_s(\bar{x})$ is given in Table II.

$\bar{x}$	n	$\Delta[\Delta E_H(n)]$	$\Delta[\Delta E_s(n)]$	$\Delta[\Delta E'_{\text{BS}}(n)]$	$[f_n - f_{\text{bulk}}]$
0.1	1	−0.0122	0.0007	+0.0000	−0.0116
	2	−0.0012	0.0000	−0.0014	−0.0001
	3	−0.0000	−0.0000	−0.0001	−0.0002
	4	−0.0001	0.0000	−0.0000	−0.0002
	5	0.0002	0.0000	−0.0001	−0.0000
	6	−0.0000	−0.0000	−0.0001	−0.0001
0.5	1	−0.0098	0.0006	+0.0011	−0.0087
	2	0.0010	0.0001	−0.0013	−0.0004
	3	0.0001	−0.0000	−0.0001	+0.0000
	4	−0.0002	0.0000	−0.0000	−0.0002
	5	0.0001	0.0000	−0.0001	−0.0000
	6	−0.0000	−0.0000	−0.0000	−0.0000
0.9	1	−0.0080	0.0005	+0.0018	−0.0068
	2	0.0008	0.0001	−0.0012	−0.0005
	3	0.0002	−0.0000	−0.0002	+0.0000
	4	−0.0002	0.0000	−0.0000	−0.0002
	5	0.0001	0.0000	+0.0000	+0.0001
	6	−0.0000	−0.0000	−0.0000	−0.0001

the same. In our pseudopotential linear-response model the surface-layer formation-energy difference is determined almost entirely by the Hartree-energy contribution which is independent of coordination number and depends only on r_s and on the position of the layer with respect to the zeroth-order electron density, $\rho^0(z)$. In Table V we give the first-layer formation-energy differences for all the alloy systems considered. Note that the magnitudes for the (110) surfaces are smaller than those for the (100) surfaces. This is due to the fact that the (110) layer spacing d is larger and thus the z coordinate of the first (110) layer, Eq. (11), is larger, and $\rho^0(z)$ deviates less from the bulk value at this position (see Fig. 1 of Ref. 14). Again, the prediction, based on the magnitudes of the formation-energy differences, that segregation will be more pronounced at the more open (100) surfaces is the same as that of the pair-bond model, but for a totally different reason.

TABLE V. First-layer formation-energy differences [see Eqs. (24) and (28)].

		Alloy		
		$Rb_{\bar{x}}K_{1-\bar{x}}$	$Cs_{\bar{x}}K_{1-\bar{x}}$ (Ry)	$Cs_{\bar{x}}Rb_{1-\bar{x}}$
	$\bar{x}$			
(100) surface	0.1	−0.0038	−0.0090	−0.0039
	0.5	−0.0033	−0.0063	−0.0033
	0.9	−0.0034	−0.0047	−0.0027
(110) surface	0.1	−0.0018	−0.0042	−0.0017
	0.5	−0.0015	−0.0027	−0.0013
	0.9	−0.0012	−0.0017	−0.0010

The nature of the layer-coupling matrix, ϕ_{nm} is illustrated in Table VI with the use of the Cs_5K_5 (100) and (110) alloy systems as examples. The qualitative features are the same for all other systems. We note first that the magnitude of ϕ_{nm} decreases rapidly as $|n-m|$ increases, and the matrix-element coupling layers near the surface differ from the bulk layer-coupling matrix elements.

The qualitative features of the layer-coupling matrix can be understood in terms of interaction potentials by including interactions out to at least the second-nearest-neighbor shell and taking the bond strengths from the calculated effective ionic interaction potentials (pair potentials). The bulk layer-coupling matrix elements are given in terms of the pair potentials by

$$\phi_{nm} = \sum_{(j)} C_{nm}^{(j)} [U_{AA}(r^{(j)}) + U_{BB}(r^{(j)}) - 2U_{AB}(r^{(j)})] , \qquad (41)$$

where the superscript (j) specifies the jth nearest-neighbor shell, $C_{n,m}^{(j)}$ is the number of jth nearest neighbors which an ion in layer n has in layer m, and $U_{\alpha\beta}(r^{(j)})$ is the value of the bulk pair potential between ions of species α and β evaluated for the jth-neighbor distance, $r^{(j)}$. The bulk pair potentials for the $Cs_{\bar{x}}K_{1-\bar{x}}$ alloys are shown in Fig. 1 (see Ref. 14 for a discussion of interaction potentials in the surface region). We get, for example, from Eq. (41) for (100) layers using the bulk Cs_5K_5 pair potentials and first- and second-nearest-neighbor interactions, $\phi_{n,n} \simeq 0.001\,58$, $\phi_{n,n\pm1} \simeq 0.002\,50$, and $\phi_{n,\pm2} \simeq 0.000\,39$, compared to the values 0.001 92, 0.003 61, and 0.000 37 given in Table VI, which were obtained from Eq. (27). It is necessary to include interactions out to at least the fifth-nearest-neighbor shell to get reasonably quantitative agreement with the exact calculation [i.e., Eq. (27)].

TABLE VI. Layer-coupling matrix $\phi_{nm}=\phi_{mn}$ for Cs_5K_5 (100) and (110) surfaces. Energy unit is e^2/k_F.

$m-n$ \ n	1	2	3	4	5	Bulk
			(100) surface			
0	0.003 29	0.001 80	0.001 96	0.001 94	0.001 90	0.001 92
1	0.003 88	0.003 48	0.003 67	0.003 61	0.003 64	0.003 61
2	0.000 50	0.000 33	0.000 39	0.000 36	0.000 38	0.000 37
3	−0.000 04	−0.000 18	−0.000 03	−0.000 01	−0.000 02	−0.000 01
4	−0.000 06	−0.0	−0.000 04	−0.000 01	−0.000 03	−0.000 02
5	−0.000 02	0.0	−0.000 01	−0.000 01	−0.000 01	−0.000 01
			(110) surface			
0	0.006 11	0.004 73	0.004 65	0.004 64	0.004 65	0.004 66
1	0.002 64	0.002 67	0.002 67	0.002 67	0.002 66	0.002 66
2	−0.000 08	−0.000 08	−0.000 08	−0.000 07	−0.000 07	−0.000 07
3	−0.000 01	−0.0	−0.0	−0.000 01	−0.000 1	−0.0
4	−0.000 02	−0.0	−0.0	−0.0	−0.0	−0.0
5	−0.000 01	−0.0	−0.0	−0.000 01	−0.0	−0.0

Since the formation-energy difference $f_n - f_{\text{bulk}}$ is very small in magnitude for $n > 2$, we may expect that the concentrations of these deeper layers will be determined primarily by the coupling between the layer concentrations. The matrix elements coupling adjacent layers are positive, thus the heat of mixing $H_m(\bar{x},\{\Delta x_n\})$ may be decreased if succeeding layers have alternately positive and negative Δx's, resulting in a nonmonotonic concentration profile. In fact, we find that in some cases, at very low temperatures, $T \ll T_D$, the "concentration layering" propagates into the bulk. This bulk layering phenomenon is an artifact of the model, resulting from the neglect of local order within and between layers and the fact that fluctuations in concentration are allowed only between layers parallel to the surface plane. The model is not valid for $T \lesssim T_D$ in any case [see the discussion following Eq. (40)].

In contrast to our pseudopotential linear-response

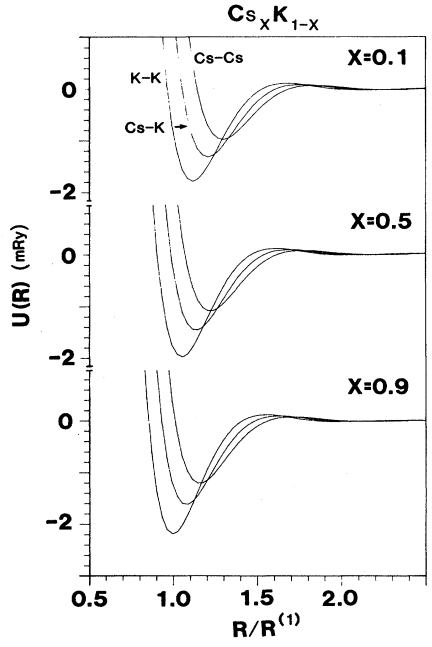

FIG. 1. Bulk pair potentials $U(R)$, as functions of interionic distance R in the $Cs_{\bar{x}}K_{1-\bar{x}}$ alloys for $\bar{x}=0.1$ 0.5, and 0.9. Energy units are 10^{-3} Ry. The distance R is in units of the bcc first-nearest-neighbor distance $R^{(1)}$; the ratios of the first five nearest-neighbor distances to $R^{(1)}$ are 1, $\sqrt{4/3}\simeq 1.15$, $\sqrt{8/3}\simeq 1.63$, $\sqrt{11/3}\simeq 1.91$, and $\sqrt{12/3}=2$, respectively.

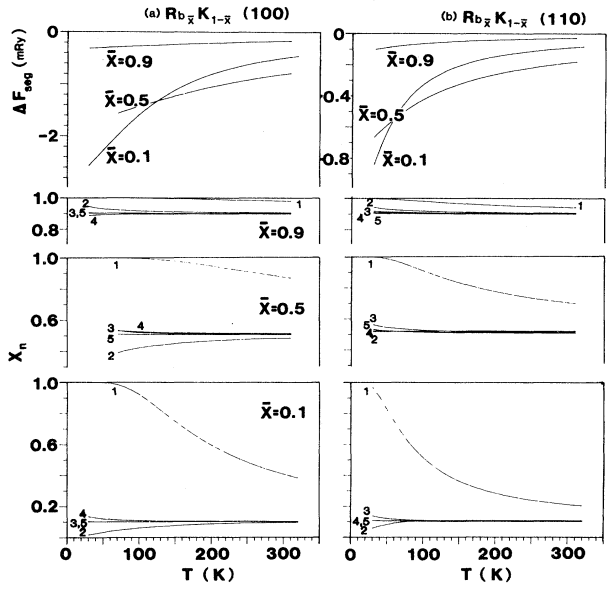

FIG. 2. Layer concentration x_n [Eq. (4)] and change in free energy upon segregation ΔF_{seg} [Eq. (29)] as functions of temperature for $Rb_{\bar{x}}K_{1-\bar{x}}$ alloys with bulk concentration $\bar{x}=0.1$, 0.5, and 0.9. Numbers 1–5 adjacent to the x_n-vs-T curves specify the layer numbers n. These results are obtained from the *pseudopotential linear-response model* explained in Secs. II A and II B with $N_s=12$ (the number of layers in the surface region).

model, the nearest-neighbor pair-bond model described in Sec. II C will always give a monotonically decreasing concentration profile if the bulk heat of mixing is positive [see Eqs. (36) and (38)]. It is possible to obtain a nonmonotonic concentration profile from a nearest-neighbor pair-bond model if the bond strengths in the surface region are adjusted[5,7]; however, this practice may be misleading since ordering may be favored in the bulk even though H_m is positive. In other words, the classification of alloys as either ordering or segregating, which is inherent to the pair-bond model, is not valid for simple metals, and is probably not valid for noble or transition metals, simply because the cohesive energy cannot be expressed as a sum over pair bonds.

C. Segregation results

In this section we present and discuss the results obtained by minimizing the free energy with respect to layer concentrations. We have included twelve layers in the surface region in each case [$N_s = 12$; see Eq. (6)]. Figures 2, 3, and 4 show the (larger) A species concentration in the first five layers of $A_{\bar{x}}B_{1-\bar{x}}$ (100) and (110) alloy systems $Rb_{\bar{x}}K_{1-\bar{x}}$, $Cs_{\bar{x}}K_{1-\bar{x}}$, and $Cs_{\bar{x}}Rb_{1-\bar{x}}$, respectively, with $\bar{x}=0.1$, 0.5, and 0.9. Results of the simple nearest-neighbor pair-bond model (Sec. II C) are shown in Fig. 5 for comparison using the $Rb_{\bar{x}}K_{1-\bar{x}}$ systems as an example. The reader is reminded that the results for temperatures near and below the disordering temperature, $T \lesssim T_D$ [Eq. (40), Table II], are probably not valid due to the neglect of local ordering within and between layers, as discussed in the preceding sections. Concentration profiles are presented in Figs. 6 and 7 as histograms of species-A concentration versus layer number at temperatures $T=250$, 200, and 150 K for the $Rb_{\bar{x}}K_{1-\bar{x}}$ (100) alloy systems; Fig. 6 gives the pseudopotential linear-response results, and Fig. 7 is obtained from the pair-bond model.

The general features of the x_n-vs-T curves are in agree-

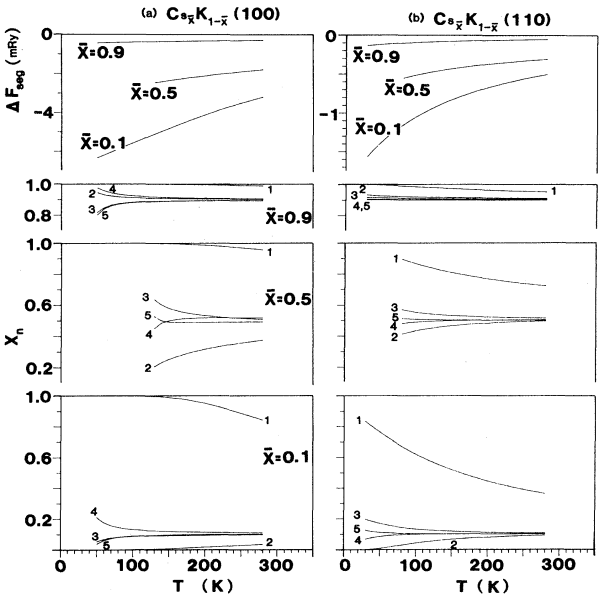

FIG. 3. Layer concentration x_n and change in free energy ΔF_{seg} as functions of temperature for $Cs_{\bar{x}}K_{1-\bar{x}}$ alloys. See caption of Fig. 2.

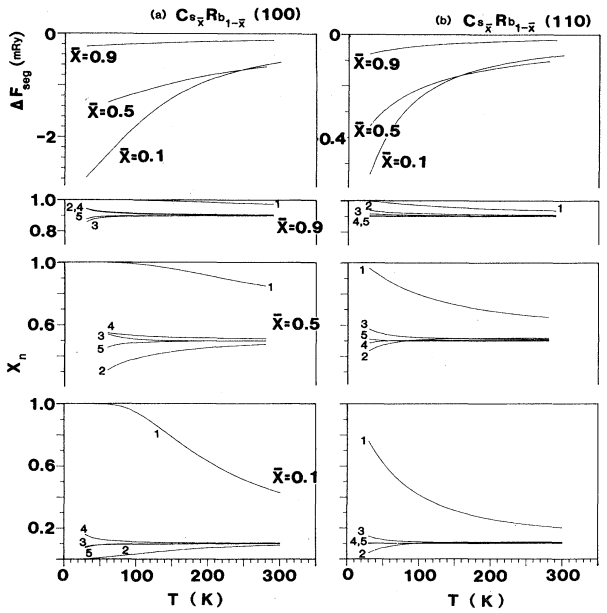

FIG. 4. Layer concentration x_n and change in free energy ΔF_{seg} as functions of temperature for $Cs_{\bar{x}}Rb_{1-\bar{x}}$ alloys. See caption of Fig. 2.

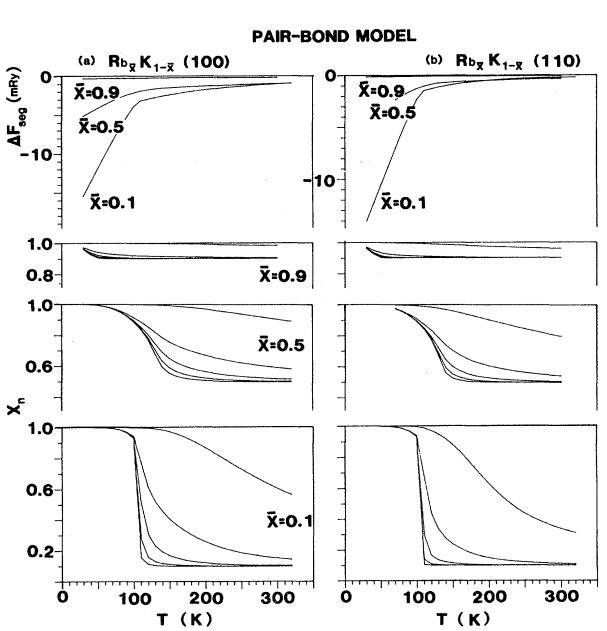

FIG. 5. Layer concentration x_n and change in free energy ΔF_{seg} as functions of temperature for $Rb_{\bar{x}}K_{1-\bar{x}}$ alloys obtained from the *pair-bond model* explained in Sec. II C. In this pair-bond model the layer concentrations decrease monotonically with increasing layer number (the x_n-vs-T curves are not labeled with layer number in this figure). See also caption of Fig. 2.

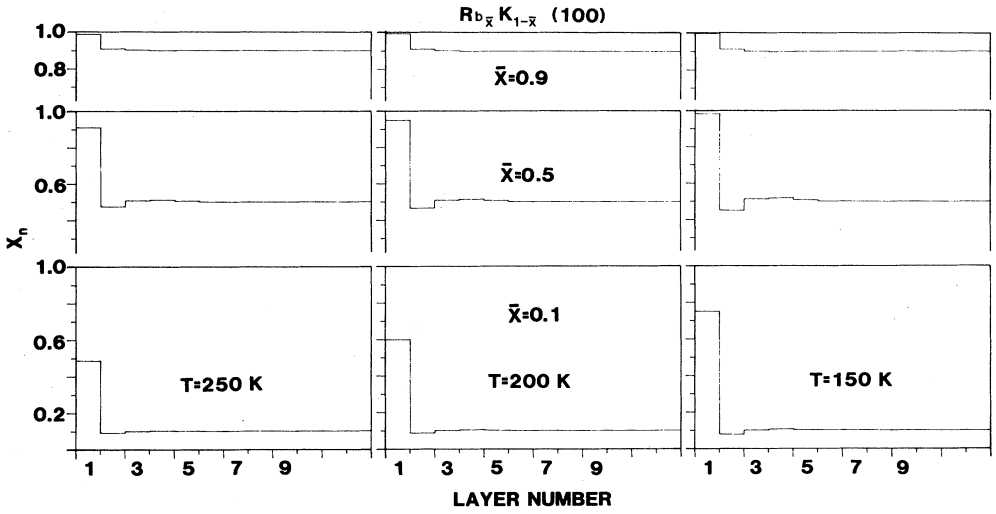

FIG. 6. Examples of layer-concentration profiles obtained from the *pseudopotential linear-response model:* the (100) surfaces of $Rb_{\bar{x}}K_{1-\bar{x}}$ alloys with bulk concentration $\bar{x}=0.1$, 0.5, and 0.9 for temperatures $T=250$, 200, and 150 K.

ment with our expectations based on the formation-energy differences $f_n - f_{\text{bulk}}$ and the layer-coupling matrix ϕ_{nm} as discussed in the preceding section:

(a) The larger (A) species always segregates to the surface layer.

(b) Segregation is more pronounced at the more open (100) surfaces and increases with decreasing temperature.

(c) Segregation is more pronounced in the $Cs_{\bar{x}}K_{1-\bar{x}}$ systems where the difference in ionic size is larger.

(d) In most cases we observe a *nonmonotonic* concentration profile—the concentration in the second layer is usually lower than the bulk concentration due to the high concentration in the first layer and the coupling between layer concentrations. However, in some cases [higher bulk concentration and/or (110) layers] the concentration profile decreases monotonically away from the surface.

(e) At very low temperatures, $T \ll T_D$ (where the model is not valid), one can see in some cases the onset of bulk concentration layering.

(f) The pair-bond model gives a monotonically decreasing concentration profile, overestimates the concentration in the surface layer, and greatly overestimates the change in free energy upon segregation.

IV. CONCLUSION

We have developed an electronic theory of surface segregation in simple-metal alloys which is based on the use of local ionic pseudopotentials and linear response, and have applied this theory to the binary simple-metal (solid solution) alloys composed of K, Rb, and Cs. We conclude that the segregation of the larger species to the surface layer is driven by single-particle terms in the total-energy expansion, i.e., by the Hartree-energy terms (first order in the pseudopotentials) which are independent

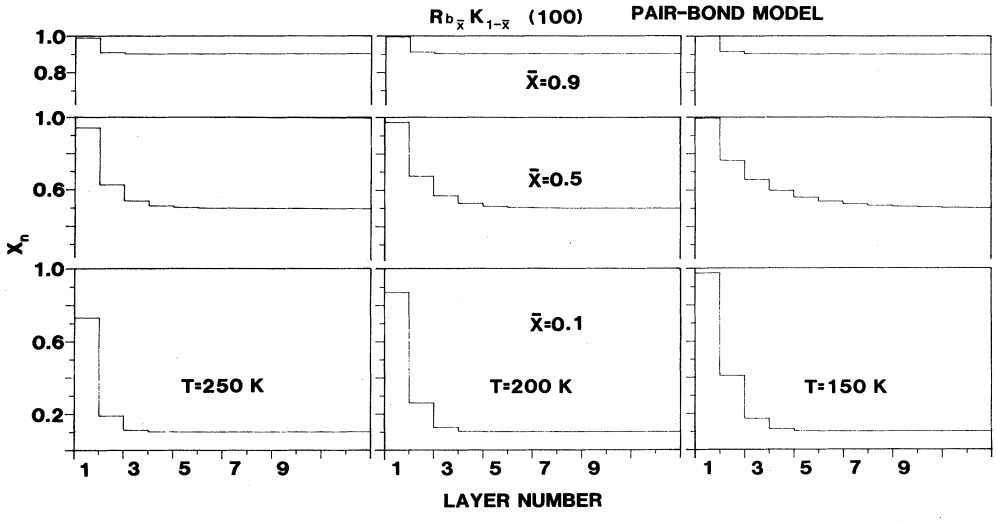

FIG. 7. Examples of layer-concentration profiles obtained from the *pair-bond model.* See also caption of Fig. 6.

of coordination number and relative positions of ions and which depend only on the position of the surface layer with respect to the inhomogenous zeroth-order electron density in the surface region. The concentration in deeper layers is determined primarily by the coupling between layer concentrations which results from interionic interactions and which may give rise to a nonmonotonic concentration profile. By comparing our electronic theory with a simple nearest-neighbor pair-bond model, in which the bond strengths are obtained from bulk thermodynamic data, we conclude that the pair-bond model is not applicable to simple-metal alloy systems, the reason being that the cohesive energy cannot be expressed as a sum over pair bonds. We speculate that the pair-bond model may not be reliable for noble- or transition-metal alloy systems for the same reason; this is supported by the results of Muscat,[10] and by the results of Connolly and Williams[31] regarding many-body interactions and the heat of mixing in transition-metal alloys. Experimental data on surface segregation in the alkali-metal systems considered in this paper is not currently available[32]; the theory can be adapted to other (nonhomovalent) simple-metal systems such as Al-Li, Al-Mg, etc., and the same mechanisms discussed here must certainly be involved.

In the current version of the theory, surface relaxation,[18] lattice distortion due to size mismatch, and effects due to local (short-range) ordering have not been considered. The inclusion of surface-relaxation and/or lattice-distortion effects would probably increase the surface-layer concentration of the larger species due to the fact that there is a greater freedom to relax the lattice in the surface region.[8] Short-range order can in principal be included using the cluster-variation method.[27,28]

ACKNOWLEDGMENTS

This work was supported by the U.S. Department of Energy under Contract No. DE-AS05-5489. We thank Dr. John Cahn and Dr. R. G. Barrera for useful discussions.

[1](a) A. Joshi, in *Interfacial Segregation,* edited by W. C. Johnson and J. M. Blakely (American Society for Metals, Metals, Park, Ohio, 1979), p. 39, and references therein; (b) J. M. McDavid and S. C. Fain, Surf. Sci. 52, 161 (1975); (c) K. Watanabe, M. Hashiba, and T. Yamoshina, *ibid.* 61, 483 (1976).

[2]D. T. Ling, J. N. Miller, I. Lindau, W. E. Spicer, and P. M. Stefan, *ibid.* 74, 612 (1978); see also Ref. 1(a).

[3]K. Wandelt and C. R. Brundle, Phys. Rev. Lett. 46, 1529 (1981); see also Ref. 1(a).

[4]H. H. Brongersma and J. M. Buck, Surf. Sci. 53, 649 (1975); H. H. Brongersma, M. J. Sparnaoy, and T. M. Buck, *ibid.* 71, 657 (1978); see also Ref. 1(a).

[5]Yee S. Ng, T. T. Tsong, and S. B. McLane, Phys. Rev. Lett. 42, 588 (1979); T. T. Tsong, Yee S. Ng, and S. B. McLane, J. Chem. Phys. 73, 1464 (1980); Yee S. Ng, T. T. Tsong, and S. B. McLane, Surf. Sci. 84, 31 (1979); see also Ref. 1(a).

[6]J. W. Gibbs, *The Collected Works of J. Willard Gibbs* (Yale University Press, New Haven, Conn., 1948), Vol. 1.

[7]F. L. Williams and D. Nason, Surf. Sci. 45, 377 (1974).

[8]F. F. Abraham, Nan-Hsiung Tsai, and G. M. Pound, Surf. Sci. 83, 406 (1979); P. Wynblatt and R. C. Ku, *ibid.* 65, 511 (1977); Y. W. Lee and H. I. Aaronson, *ibid.* 95, 227 (1980).

[9]G. Kerker, J. L. Moran-Lopez, and K. H. Bennemann, Phys. Rev. B 15, 683 (1977); P. H. Lambin and J. P. Gaspard, J. Phys. F 10, 2413 (1980).

[10]J. P. Muscat, J. Phys. C 15, 867 (1982).

[11]See B. L. Györffy and G. M. Stocks, in *Electrons in Disordered Metals and at Metallic Surfaces,* edited by P. Phariseau, B. L. Györffy, and L. Scheire (Planum, New York, 1979).

[12]F. Gautier, F. Ducastelle, and J. Giner, Philos. Mag. 31, 1373 (1975).

[13]M. Shlüter and C. M. Varma, Phys. Rev. B 23, 1633 (1981); T. Soma, H. Matsuo and M. Funaki, Phys. Status Solidi B 108, 221 (1981); T. Soma, H. Matsuo, and Y. Kohbu, *ibid.* 107, 761 (1981); R. N. Singh, J. Phys. F 11, 389 (1981).

[14]R. N. Barnett, R. G. Barrera, C. L. Cleveland, and Uzi Landman, Phys. Rev. B 28, 1667 (1983).

[15]D. Stroud, in *Theory of Alloy Phase Formation,* edited by L. H. Bennett (TMS-AIME, Warrendale, Penn., 1980), p. 84.

[16]N. D. Lang and W. Kohn, Phys. Rev. B 1, 4555 (1970).

[17]K. S. Singwi, A. Sjölander, M. P. Tosi, and R. H. Land, Phys. Rev. B 1, 1044 (1970).

[18]R. N. Barnett, Uzi Landman, and C. L. Cleveland, Phys. Rev. B 28, 1685 (1983); R. N. Barnett, Uzi Landman, and C. L. Cleveland, *ibid.* 27, 6534 (1983).

[19]J. E. Inglesfield, J. Phys. C 2, 1285 (1969).

[20]P. S. Ho, Phys. Rev. 169, 523 (1968).

[21]Z. D. Popovic, J. P. Carbotte, and G. R. Piercy, J. Phys. F 4, 351 (1974).

[22]Charles Kittel, *Introduction to Solid State Physics,* 4th ed. (Wiley, New York, 1971), pp. 96 and 101, and references therein.

[23]L. A. Girifalco, Acta. Metall. 24, 759 (1976).

[24]Mark O. Robbins and L. M. Falicov, Phys. Rev. B 25, 2343 (1982); see also Ref. 13.

[25]M. P. Iñiguez and J. A. Alonso, J. Phys. F 11, 2045 (1981).

[26]T. Yokokawa and O. J. Kleppa, J. Chem. Phys. 40, 46 (1964).

[27]M. Kurata, R. Kikuchi, and T. Watari, J. Chem. Phys. 21, 434 (1953).

[28]J. L. Morán-López and L. M. Falicov, Phys. Rev. B 18, 2542 (1978); B 18, 2549 (1978); V. Kumar, D. Kumar, and S. K. Joshi, *ibid.* 19, 1954 (1979).

[29]M. Hansen, *Constitution of Binary Alloys* (McGraw-Hill, New York, 1958); R. P. Elliot, *Constitution of Binary Alloys, First Supplement* (McGraw-Hill, New York, 1965); F. A. Shunk, *Constitution of Binary Alloys, Second Supplement* (McGraw-Hill, New York, 1969).

[30]U. Shmueli, V. Steinberg, T. Sverbilova, and A. Voronel, J. Phys. Chem. Solids 42, 19 (1981); V. Steinberg, T. Sverbilova, and A. Voronel *ibid.* 42, 23 (1981).

[31]J. W. D. Connolly and A. R. Williams, Phys. Rev. B 27, 5169 (1983).

[32]See, however, G. L. Powell, R. E. Clausing, and G. E. McGuire, Surf. Sci. 49, 310 (1975), where Na segregation to Li surfaces is reported, and J. Kojnik, A. Szász, L. Kertész, and A. S. Solakov, Phys. Status Solidi A 72, 131 (1982), regarding Mg segregation in Al-Mg alloys.